AD

TECHNICAL REPORT ARBRL-TR-02261

ENERGY TRANSFER AND QUENCHING RATES OF LASER-PUMPED ELECTRONICALLY EXCITED ALKALIS IN FLAMES

John E. Allen, Jr.
William R. Anderson
David R. Crosley
Todd D. Fansler

August 1980

US ARMY ARMAMENT RESEARCH AND DEVELOPMENT COMMAND
BALLISTIC RESEARCH LABORATORY
ABERDEEN PROVING GROUND, MARYLAND

Destroy this report when it is no longer needed.
Do not return it to the originator.

Secondary distribution of this report by originating or sponsoring activity is prohibited.

Additional copies of this report may be obtained from the National Technical Information Service, U.S. Department of Commerce, Springfield, Virginia 22151.

The findings in this report are not to be construed as an official Department of the Army position, unless so designated by other authorized documents.

The use of trade names or manufacturers' names in this report does not constitute indorsement of any commercial product.

REPORT DOCUMENTATION PAGE

READ INSTRUCTIONS BEFORE COMPLETING FORM

1. REPORT NUMBER: TECHNICAL REPORT ARBRL-TR-02261
2. GOVT ACCESSION NO.:
3. RECIPIENT'S CATALOG NUMBER:

4. TITLE (and Subtitle): ENERGY TRANSFER AND QUENCHING RATES OF LASER-PUMPED ELECTRONICALLY EXCITED ALKALIS IN FLAMES

5. TYPE OF REPORT & PERIOD COVERED: BRL Technical Report

6. PERFORMING ORG. REPORT NUMBER:

7. AUTHOR(s): JOHN E. ALLEN, JR.,* WILLIAM R. ANDERSON, DAVID R. CROSLEY**, TODD D. FANSLER***

8. CONTRACT OR GRANT NUMBER(s):

9. PERFORMING ORGANIZATION NAME AND ADDRESS
U.S. Army Armament Research & Development Command
U.S. Army Ballistic Research Laboratory
ATTN: DRDAR-BL
Aberdeen Proving Ground, MD 21005

10. PROGRAM ELEMENT, PROJECT, TASK AREA & WORK UNIT NUMBERS: 1L161102AH43

11. CONTROLLING OFFICE NAME AND ADDRESS
U.S. Army Armament Research & Development Command
U.S. Army Ballistic Research Laboratory
ATTN: DRDAR-BLP
Aberdeen Proving Ground, MD 21005

12. REPORT DATE: Aug 80

13. NUMBER OF PAGES: 40

14. MONITORING AGENCY NAME & ADDRESS (if different from Controlling Office):

15. SECURITY CLASS. (of this report): UNCLASSIFIED

15e. DECLASSIFICATION/DOWNGRADING SCHEDULE:

16. DISTRIBUTION STATEMENT (of this Report)

Approved for public release; distribution unlimited.

17. DISTRIBUTION STATEMENT (of the ebstract entered in Block 20, if different from Report)

18. SUPPLEMENTARY NOTES

*NAS-NRC Resident Research Associate; present address: Goddard Space Flight Center Greenbelt, MD 20770

**Molecular Physics Laboratory, SRI International, Menlo Park, CA 94025

***Engine Research Div., General Motors Research Lab, Warren, MI 48090

19. KEY WORDS (Continue on reverse side if necessary and identify by block number)

Combustion
Energy transfer
Laser excitation
Alkali atoms
Fluorescence
Optoacoustic effect

20. ABSTRACT (Continue on reverse side if necessary and identify by block number) (clt)

A pulsed, tunable dye laser has been used to excite each of the 3p, 3d, 4p, 5s and 4d levels of sodium atoms seeded into an atmospheric pressure acetylene-air flame. Three of these transitions, 3d, 5s and 4d, involve two-photon absorption from the ground 3s state. Fluorescence measurements furnish the populations of each of the levels populated by collisional transfer, enabling the deduction of relative energy transfer and quench rates among the four higher states. Fluorescence and opto-acoustic measurements under conditions near

(continued on reverse side)

20. ABSTRACT (Cont'd)

optical saturation of the 3p transition yield energy transfer rates and quenching rates for the two doublet components. Total collision-broadened linewidths are obtained by scanning the laser in a narrow-line mode. A qualitative experiment seeding the flame with both sodium and lithium suggests the presence of electronic-to-vibrational-to-electronic energy transfer.

TABLE OF CONTENTS

LIST OF ILLUSTRATIONS

LIST OF TABLES

I. INTRODUCTION

There is considerable experimental evidence demonstrating the existence of major departures from thermal equilibrium in the reaction zone of a variety of flames[1]. In addition, recent results confirm the non-equivalence of different forms of energy, electronic, vibrational, rotational and translational, in their ability to affect chemical reaction rates[2]. Thus a system in thermal disequilibrium may well have reaction rates (even mechanisms) not describable by simple Arrhenius parameters obtained from measurements at low temperature. How much these considerations affect actual overall combustion processes is currently unknown. The answers lie in attaining, at least for one or a few simple systems, a full understanding of the chemistry in this context: knowledge of reaction rates of excited states, and of the mechanisms and rates of interconversion of energy among the several possible degrees of freedom. Even for a combustion environment in which the chemistry can be successfully described by a single temperature parameter, considerations of energy transfer remain important. Most of the new laser-based diagnostic techniques measure population distributions for internal degrees of freedom of various molecules, and these observables must in turn be related to the pertinent chemical kinetic and gas dynamic temperature.

To date there exists little, if any, direct experimental investigation of rates and mechanisms of the transfer of energy within a flame system. In this series of experiments, we explore a number of aspects of these phenomena in an atmospheric pressure, acetylene/air flame. To do so, the flame is seeded with Na (and sometimes Li), as done by those practiced in the technique of line reversal thermometry. In that method, one strives to attain thermal equilibrium between the Na and the flame gases; here, on the contrary, we use a pulsed tunable dye laser to purposely perturb the populations of various excited levels of the Na far from their thermal equilibrium values. Measurements are made of Na fluorescence dispersed through a monochromator, and of the pulsed pressure waves[3] formed by collisional quenching. The laser is operated at power levels corresponding to non-linear as well as linear regimes of absorption. Within the framework of steady-state collision kinetics, the data furnish a variety of relative and absolute rates for state-to-state energy transfer and overall quenching.

---

[1] *A. G. Gaydon and H. G. Wolfhard, Flames, 3rd ed., Chapman and Hall, 1970.*

[2] *P. R. Brooks and E. F. Hayes, editors, State-to-State Chemistry, Amer. Chem. Soc. Symposium Series 56, 1977.*

[3] *J. E. Allen, W. R. Anderson, and D. R. Crosley, "Opto-Acoustic Pulses in a Flame", Optics Lett. 1, 118-120 (1977).*

Such information is important in itself, to properly describe the excitation and quenching mechanisms operative in Na, for experiments such as the line reversal technique itself and the use of laser-excited fluorescence in Na as a flame probe. In particular the experiments involving excitation under conditions of high laser intensity are pertinent to the development of saturation techniques[4] in laser excited fluorescence. This is a promising way of overcoming the problem of quenching in the employment of laser excited fluorescence as a probe of molecules present in combustion systems; information on a simple system such as Na is necessary to better understand the physics of the saturation process itself under real flame conditions.

Of perhaps more importance, however, is the information obtained not on the Na per se but on the behavior of the collision partner flame gases through a study of the Na transfer. In this connection, we emphasize at the outset that we have not carried out the current measurements over a range of flame parameters; in fact, we have not laboured in the current work to obtain an especially well characterized flame. Such work is clearly the next step beyond these experiments. Nonetheless, the present results do provide some insights into energy transfer mechanisms. In particular we find: stepwise relaxation in a multilevel system, but not in a way prescribed by a simple pattern; a collisional conversion of electronic to translational energy varying in efficiency with energy; and the occurrence of electronic to vibrational to electronic energy transfer. All of these results have implications concerning understanding the flow of energy among degrees of freedom in a complex flame environment.

Figure 1 exhibits the energy level scheme for Na pertinent to these experiments. The vertical solid lines denote the pumping transitions. In the case of the (parity-forbidden) 4d-3s, 5s-3s, and 3d-3s transitions, atoms are excited by two-photon absorption at a frequency $\nu = (\frac{1}{2})(\Delta E/h)$. Excitation of the 4p and 3p levels is accomplished by single-photon absorption.

The slanted dashed lines in Figure 1 denote the transitions monitored through the spectrometer. These pumping and monitoring wavelengths are listed in Table I. Also included in Figure 1 are several nearby levels (4s, 4f, 5p and 6s) which are not monitored and which are ignored in the kinetic network, as well as an indication of the magnitude of kT for 2545°K, the adiabatic flame temperature for a stoichiometric acetylene-air flame[1].

---

[4] *J. W. Daily, "Saturation Effects in Laser Induced Fluorescence Spectroscopy", Appl. Opt. 16, 568 (1977).*

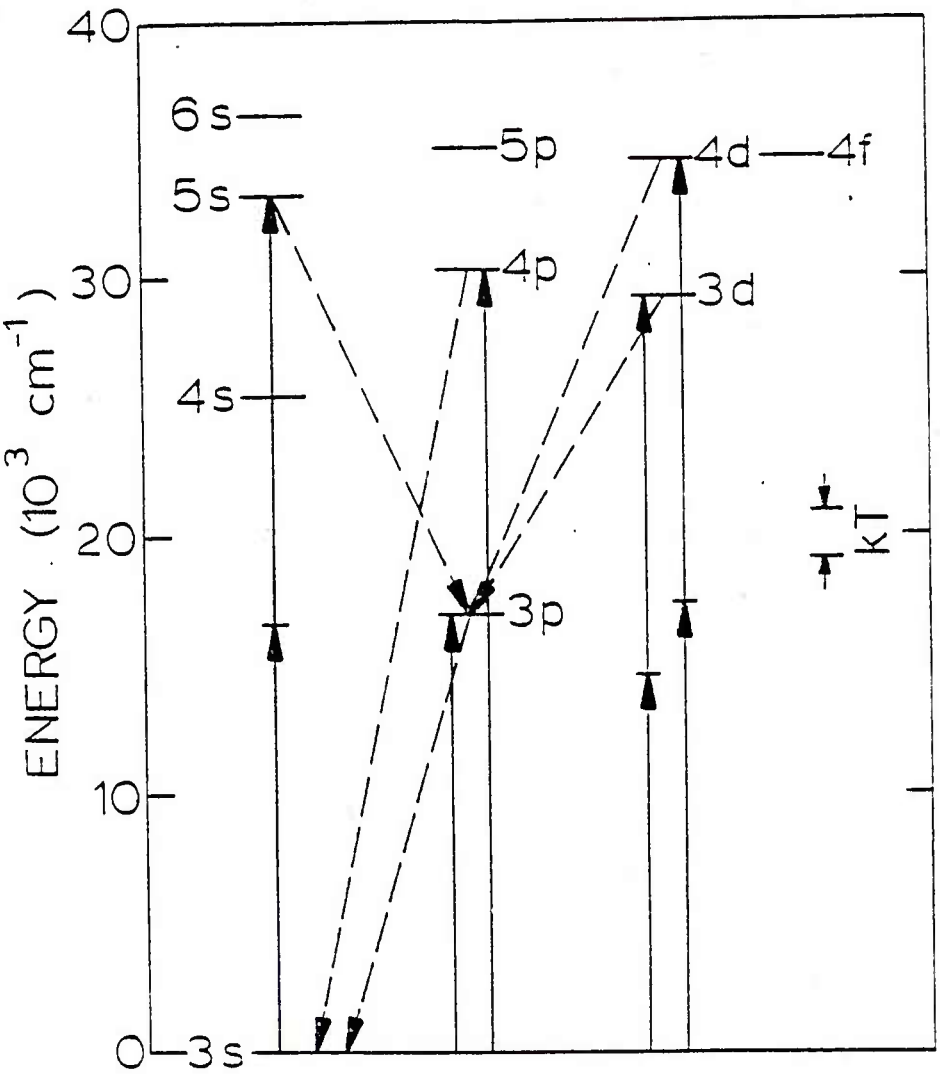

Figure 1. Energy levels of and transitions in Na pertinent to the experiments. The solid vertical lines denote individual excitations routes, while the slanted, dashed lines indicate observation transitions (numerical values are given in Table 1). The 4s, 4f, 5p and 6s levels are neither pumped nor monitored but included here for reference. The value of KT shown is that for the flame temperature.

TABLE 1. EXCITATION AND OBSERVTION WAVELENGTHS FOR Na

LEVEL	ENERGY, CM^{-1}	EXCITATION WAVELENGTH A	NUMBER OF PHOTONS TO EXCITE	MONITOR WAVELENGTH, A	MONITOR TRANSITION
3p	16970	5890,5896	1	5890,5896	3p-3s
3d	29170	6854	2	8191	3d-3p
4p	30270	3303	1	3303	4p-3s
5s	33200	6022	2	6159	5s-3p
4d	34550	5787	2	5686	4d-3p

II. EXPERIMENTAL DETAILS

The basic experimental arrangement, which is the same for all of the measurements, is described here; individual details are included in the sections which follow.

A fuel rich mixture (about 1.5 x stoichiometric) of acetylene and air is burned on a standard flame aspirator burner at atmospheric pressure. Na is seeded into the flame as sodium iodide solution. A pulsed, flash-lamp-pumped dye laser (Chromatix CMX4) is directed into the flame to provide resonant pumping of a particular Na excited state. The laser is operated in the visible (with the dyes rhodamine 6G or rhodamine 640); for the 4p-3s absorption, frequency doubling is used. Insertion of an intracavity etalon permits the laser linewidth to be narrowed from its nominal 7 cm^{-1} full-width at half-maximum (FWHM) to a FWHM of 0.3 cm^{-1}. The laser pulse length is 0.9 μsec, and the laser is capable of modest power - a few mJ per pulse. Nearly all of the experiments are carried out at repetition rates of 10 or 15 pulses per second.

The laser beam enters the flame at a 45° angle with respect to the burner slot. For those experiments requiring precise knowledge of the laser spectral power density, an iris is used to vignette the beam, providing a spatially homogeneous cross section, and the beam diameter and profile are measured using a knife-edge on a translational stage[5]. For the two-photon absorption experiments, which require high laser power, the beam is focussed with a 15 cm focal length lens. Typical beam diameters were 4 mm (unfocussed) and 0.2 mm (focussed). The burner was raised or lowered with respect to the laser beam for runs at different heights.

Measurements are made of the fluorescence from the excited states of Na, due to the laser pumping. The region of the flame irradiated by the laser is focussed onto the slit of a 0.35 m monochromator outfitted with an EMI 9859QA photomultiplier; the response of the detection system is calibrated using a standards lamp. Due to the pulsed nature of the laser, the laser-induced signal is typically less than the background thermal flame emission on an average basis although it is much higher during the actual laser pulse. This is especially a problem when the intense 3p-3s transition is monitored; occasionally an attenuating optical filter must be placed in front of the slit to prevent saturation of the photomultiplier. The use of gated detection thus greatly improves the signal-to-noise ratio. The photomultiplier output is fed through a pre-amplifier and precision attenuator into a boxcar integrator which has a 0.5 μsec gate width and is triggered by a synchronization pulse from the laser. The boxcar output, which is the average signal over a number of laser pulses, forms the input to a chart recorder. In addition, the

---

[5] *H. D. Zeman, Electron and Photon Interactions with Atoms, (H. Kleinpoppen and M. R. C. McDowell, editors), p. 581, Plenum Press, 1976.*

instantaneous photomultiplier response is monitored on an oscilloscope, also triggered by the synchronization pulse.

Although some of the Na atoms fluoresce, most (> 95%) are quenched by collisions with the flame gases. In at least the case when the 3p level is pumped, the absorbed laser energy is converted to translational energy of the flame gases, presumably by E→V→T transfer, resulting in the formation of pulsed pressure waves (sound waves) which propagate outward from the flame[3]. These are monitored using a condenser microphone, typically 1.3 cm diameter, situated a few cm from the flame. Its output after appropriate preamplification and attenuation, is fed to the boxcar and oscilloscope.

The laser power is varied by inserting neutral density filters into the beam. These filters are calibrated using the laser and a thermopile. The amount of absorption, by the Na, of the laser beam passing through the flame is measured using a laser power meter while scanning the laser wavelength.

A. Transfer Among Highly Excited States

In this series of experiments, the laser pumps, in turn, each of the four excited states lying in the 30,000 to 35,000 cm^{-1} region (see Figure 1 and Table 1). The population of each of the four levels is deduced from measurements of the laser-induced emission intensity for a line originating from that level. From the population ratios we determine ratios of the total quench rates and the energy transfer rates among these levels.

Consider, for illustrative purposes, the case in which the 5s level is pumped by the two-photon transition at 6022 A. The populations of the three levels not initially excited are given, within the steady-state approximation, by the following equations:

$$\frac{dN(4d)}{dt} = 0 = k(5s\rightarrow 4d)N(5s) + k(4p\rightarrow 4d)N(4p)$$

$$+ k(3d\rightarrow 4d)N(3d) - Q(4d)N(4d)$$

$$\frac{dN(4p)}{dt} = 0 = k(4d\rightarrow 4p)N(4d) + k(5s\rightarrow 4p)N(5s)$$

$$+ k(3d\rightarrow 4p)N(3d) - Q(4p)N(4p)$$

$$\frac{dN(3d)}{dt} = 0 = k(4d \rightarrow 3d)N(4d) + k(5s \rightarrow 3d)N(5s)$$

$$+ k(4p \rightarrow 3d)N(4p) - Q(3d)N(3d)$$

(when any other level is pumped, there is a corresponding equation for dN(5s)/dt). Here, N(i) is the population of level i, and k(i→j) is the transfer rate from level i to level j. Q(i) is the total loss rate from level i; it is equal to the sum of the rates of all the collisional transfer processes out of level i, the total radiative rates out of level i, and the rates of any reactive collisions involving level i and the flame gases. Detailed balancing is invoked to relate upward and downward transfer rates:

$$k(i \rightarrow j) = k(j \rightarrow i) \quad (g_j/g_i) \exp [(E_j - E_i)/KT],$$

where g_i is the degeneracy of level i. This leaves a total of ten independent rates in the full network of equations: the six downward transfer rates among the four levels, and the four quench rates.

Three important assumptions are implicit in the use of these equations. The first is that the 3p level can be decoupled from these four excited states. This is valid insofar as upward transfer (e.g., 3p→4p) is negligible, which is reasonable in view of the large energy difference between 3p and the levels considered here. The second, which is more tenuous, is the omission of the 4s, 5p and 6s levels, which are much closer. Experimentally, we see no emission from 5p for any pumping transition, and only a very small amount from 6s in one case (pumping 4p). Thus the population of these levels is probably negligible, and their neglect is valid. However, our instruments are incapable of detecting transitions originating from 4s and we have no information on the population of this level.

The third assumption concerns our handling of the 4f level, whose transitions we also cannot detect. It lies within 40 cm^{-1} of the 4d level. We assume very rapid transfer between 4d and 4f, so that the net result is that of a single level (which we continue to designate 4d) having the same energy but 12/5 the degeneracy of the 4d alone. It is our opinion that this limit of complete 4d-4f mixing is more realistic than the opposite limit of no mixing. (An analysis of the data using this latter no-mixing limit yields some different quantitative results but the same qualitative conclusions.)

The data are taken by holding the laser frequency constant at the peak of the appropriate absorption line, and scanning the spectrometer

over the four fluorescence lines. Large slit widths, 500 or 1000μ, are typically used. Figure 2 shows a scan of the 4d-3p and 5s-3p lines upon excitation of the 5s level. The intensities S are determined from the area under each scan, and reduced to relative populations through

$$N(i) = S(i)/A_i \eta(\lambda)$$

where A_i is the Einstein emission coefficient for the corresponding line (taken from the compilation by Wiese, Smith, and Miles[6]), and $\eta(\lambda)$ is the spectrometer-detector efficiency at the wavelength of the line. The population ratios so obtained are collected in Table 2.

These twelve data can then be used, in principle, with the twelve steady-state equations as a slightly overdetermined set for the ten unknown rates. In practice, the equations form an ill-conditioned set due to the ability to set only upper limits for two ratios using the 3d pump, and the two very low ratios using the 4p pump. Consequently, we choose to use nine equations to solve for nine unknowns as ratios to the rate of total loss from the 4p level, Q(4p), which is set equal to 1. The results of this procedure are displayed in Table 3.

Now an important self-consistency check on the results is that the sum of the state-to-state rates measured for each level be less than the total loss rate measured, e.g., that

$$k(5s \rightarrow 4d) + k(5s \rightarrow 4p) + k(5s \rightarrow 3d) < Q(5s) \quad .$$

This must be true since Q(i) is the sum of the measured rates plus radiative loss, possible reactive loss, and transfer to the lower-lying 4s, 3p and 3s levels. The ratios of the sum of the measured rates to the total loss rate are given in Table 4. These values in general exhibit the desired consistency; the ratio for the 5s level is equivalent to 1 within the uncertainties. In addition, there is a definite trend to a lower ratio with lower energy of the level. Thus a large fraction of the transfer out of 4d and 5s is to levels in the near vicinity, with very little direct quenching to 3s or even 3p. On the other hand, since upward transfer from 4p or 3d is not rapid (see Table 3), the bulk of the loss from these levels is to 3s, 3p, 4s or by radiation or reaction.

One may thus infer that a highly excited Na atom, as in the 4d or 5s level, returns to the ground 3s state not by a single collision but in a stepwise fashion through 4p or 3d, probably then via 3p to 3s. This loss of energy in several smaller steps is in accord with a view of

---

[6] *W. L. Wiese, M. W. Smith and B. M. Miles, Atomic Transition Probabilities, Vol. II, p. 2, U.S. Government Printing Office, 1969.*

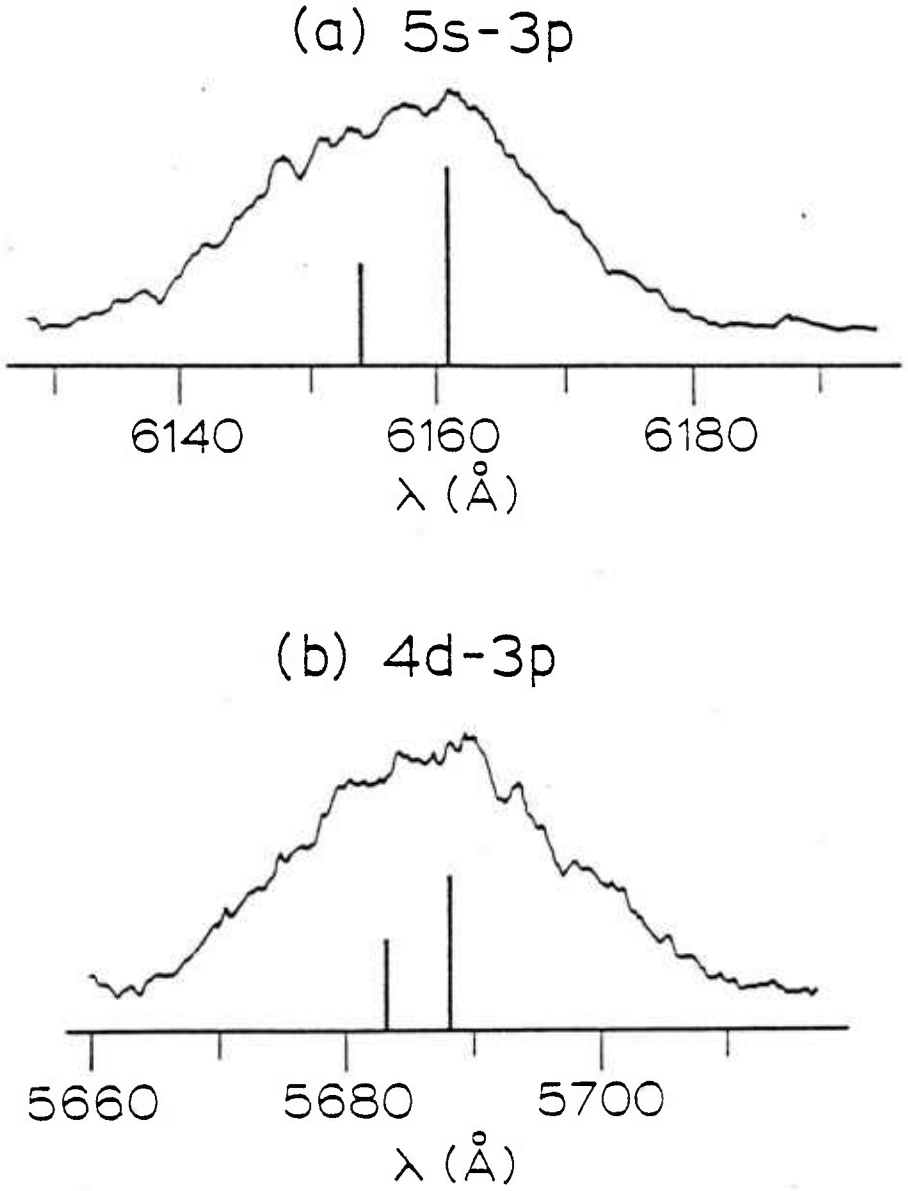

Figure 2. Spectrometer scans, using 1000 μ slits, of the laser-induced fluorescence for (a) 5s-3p and (b) 4d-3p, following initial excitation of 5s. The stick spectra underneath the scans correspond to the fully resolved fine-structure components in each line.

TABLE 2. POPULATION RATIOS FOR HIGHLY EXCITED STATES

LEVEL PUMPED	RATIO	VALUE
4d	N(5s)/N(4d)	0.15
	N(4p)/N(4d)	0.40
	N(3d)/N(4d)	0.71
5s	N(4d)/N(5s)	0.23
	N(4p)/N(5s)	0.37
	N(3d)/N(5s)	0.55
4p	N(4d)/N(4p)	0.022
	N(5s)/N(4p)	0.008
	N(3d)/N(4p)	0.14
3d	N(4d)/N(3d)	<0.013
	N(5s)/N(3d)	<0.038
	N(4p)/N(3d)	0.13

TABLE 3. ENERGY TRANSFER AND TOTAL LOSS RATES FOR HIGHLY EXCITED STATES

TOTAL LOSS	
Q(4d)	3.6
Q(5s)	2.1
Q(4p)	1*
Q(3d)	3.9

DOWNWARD TRANSFER	
k(4d→5s)	0.32
k(4d→4p)	0.38
k(4d→3d)	2.52
k(5s→4p)	0.09
k(5s→3d)	0.64
k(4p→3d)	0.42

UPWARD TRANSFER**	
k(5s→4d) = 5.83 k(4d→5s)	1.76
k(4p→4d) = 0.370 k(4d→4p)	0.13
k(3d→4d) = 0.120 k(4d→3d)	0.29
k(4p→5s) = 0.064 k(5s→4p)	0.006
k(3d→5s) = 0.021 k(5s→3d)	0.013
k(3d→4p) = 0.323 k(4p→3d)	0.14

* All values normalized to Q(4p) = 1.

** Constrained by detailed balancing, at 2545°K, to ratios indicated. The level designated 4d includes as well the nearby 4f, with a total degeneracy of 12.

TABLE 4. RATIOS OF MEASURED STATE-TO-STATE RATES TO TOTAL LOSS RATE

LEVEL	RATIO
4d	0.89
5s	1.16
4p	0.56
3d	0.11

the Na electronic energy transferring into vibrational levels of the flame gases (N_2, which constitutes the majority gas, has a vibrational spacing of 2360 cm^{-1}). Such stepwise relaxation, with significant population of intermediate states, clearly has implications for the flame chemistry, particularly where some highly excited reactive species is formed as the nascent product in an exoergic prior reaction.

B. Transfer in and Quenching of 3^2P

Here we use the laser to resonantly pump, in turn each of the 3^2p fine structure levels. Spectrometer scans of the resolved emission lines yield the degree of collisional population transfer between the two levels. With the laser operated near optical saturation of the 3s-3p transitions, we also measure the fluorescence intensity as a function of laser power. These data are sufficient to yield the absolute transfer rate between and individual quenching rates for the two fine structure levels.

Additionally, we measure the magnitude of the opto-acoustic pulses[3] generated upon pumping each state. Following resonant excitation, collisional transfer of electronic energy into vibrational levels of the flame gases and ultimate conversion into translational energy forms a pressure wave. The output of the microphone as a function of laser frequency is shown in Figure 3, clearly demonstrating that this is a net E↦T process. When relatively high concentrations of NaI are used in the aspirated solution, these pulsed sound waves are readily audible to an observer within 1-2 meters of the burner, and listening for them is routinely used in initial tuning of the laser to the resonance lines. Knowledge of the absorbed laser energy per pulse, and an estimate of the heat capacity of the flame gases, indicates that the region illuminated by the laser undergoes a translational temperature increase of the order of 1°K, which is in accord with the measured pressure amplitudes at the microphone of $\sim$ 100 mTorr. Thus the opto-acoustic pulses should perturb neither the chemical kinetics nor the gas dynamics.

We now consider a description of the three level 3p-3s system near optical saturation of one of the transitions. Level 1 is 3^2S, level 2 is $3^2P_{1/2}$, and level 3 is $3^2P_{3/2}$. For the case in which the laser pumps level 3, the steady state approximation yields for the input/output balance to that level

$$B_{13}IN_1 + T_{23}N_2 = (B_{31}I + A_{31} + T_{32} + Q_{31})\, N_3 \qquad (1)$$

where B and A are Einstein coefficients and I is the laser intensity. T is the ^2P fine structure collisional transfer rate; by detailed balancing $T_{23} = 1.98\ T_{32}$ at 2545°K. Q_{31} is the quench rate for level 3, and N_i is the population of level i. Level 2 has a population described, for initial excitation to level 3, by

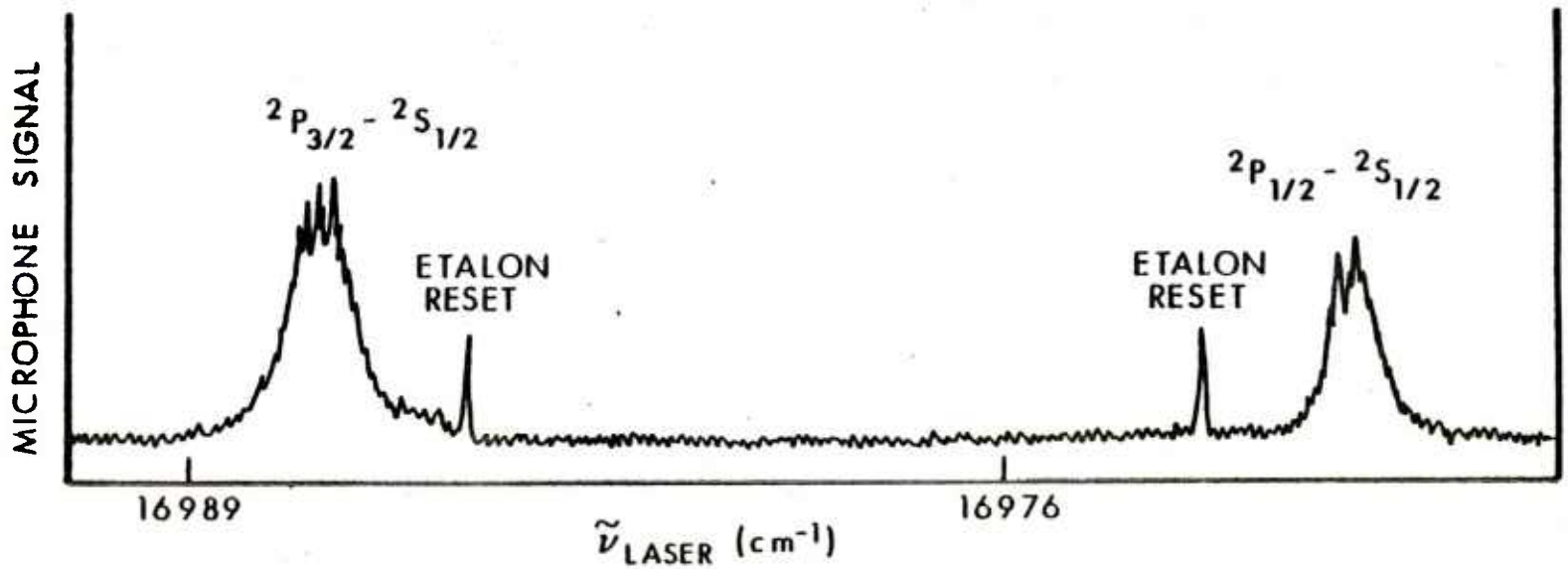

Figure 3. Opto-acoustic pulse signal as a function of laser frequency. The laser here has a bandwidth of 0.16 cm^{-1} and is scanned over the region including both doublet components. The laser frequency scale is here offset from the true frequency by ~ 10 cm^{-1}. The spikes marked 'etalon reset' are artifacts of the automatic scanning operation.

$$T_{32}N_3 = (A_{21} + Q_{21} + T_{23})\, N_2, \qquad (2)$$

so that the ratio $R_3 = N_2/N_3$ is independent of I. The total Na population is a constant, N_0, so that

$$N_1 = N_0 - N_2 - N_3 \qquad (3)$$

to a good approximation. In addition, we need the ratio $R_2 = N_3/N_2$ when level 2 is pumped; it is obtained from

$$T_{23}N_2 = (A_{31} + Q_{31} + T_{32})\, N_3. \qquad (4)$$

Now the fluorescence signal S_3 from level 3 is proportional to $A_{31}N_3$. Combining Equations (1), (2) and (3) yields for S_3 as a function of I

$$S_3 \propto IB_{13}A_{31}N_0/[(R_3 + B_{31}/B_{13} + 1)IB_{13} + A_{31} + Q_{31} + T_{32} - R_3T_{23}].$$

It is convenient to invert this equation:

$$S_3^{-1} \propto [R_3 + B_{31}/B_{13} + 1] + [A_{31} + Q_{31} + T_{32} - R_3T_{23}]/IB_{13}. \qquad (5)$$

Thus, a plot of S_3^{-1} vs. I^{-1} should yield a straight line. The Einstein coefficients are related by $B_{ij} = (g_j/g_i)B_{ji}$, and $B_{ji} = (\lambda^3/2hc)A_{ji}$, and R_3 is separately measured. The slope-to-intercept ratios from Equations (5), and from a similar expression for S_2^{-1} vs. I^{-1}, together with Equations (3) and (4), furnish four data from which can be extracted the ratios of the three unknowns T_{32}, Q_{31} and Q_{21}, to the radiative lifetime $\tau = A_{31}^{-1} = A_{21}^{-1}$. τ is known independently,[6] so that absolute transfer and quenching rates may be obtained.

The opto-acoustic pulse signal $M \propto Q_{31}N_3 + Q_{21}N_2$ may be treated in a similar way. For a population ratio R_3 near the equilibrium value of 0.505, the equations predict a slope-to-intercept ratio from Equation (5) of 0.67 times the slope-to-intercept ratio of a plot of M^{-1} vs. I^{-1}. In a series of experiments over a wide range of Na concentration, we find a ratio 0.65 ± 0.09, confirming the predicted behavior.

In Figure 4 are shown spectrometer scans of the laser-induced fluorescence for pumping each of the ^2P levels. From such scans the ratios R_3 and R_2 are obtained. The results for a series of runs at

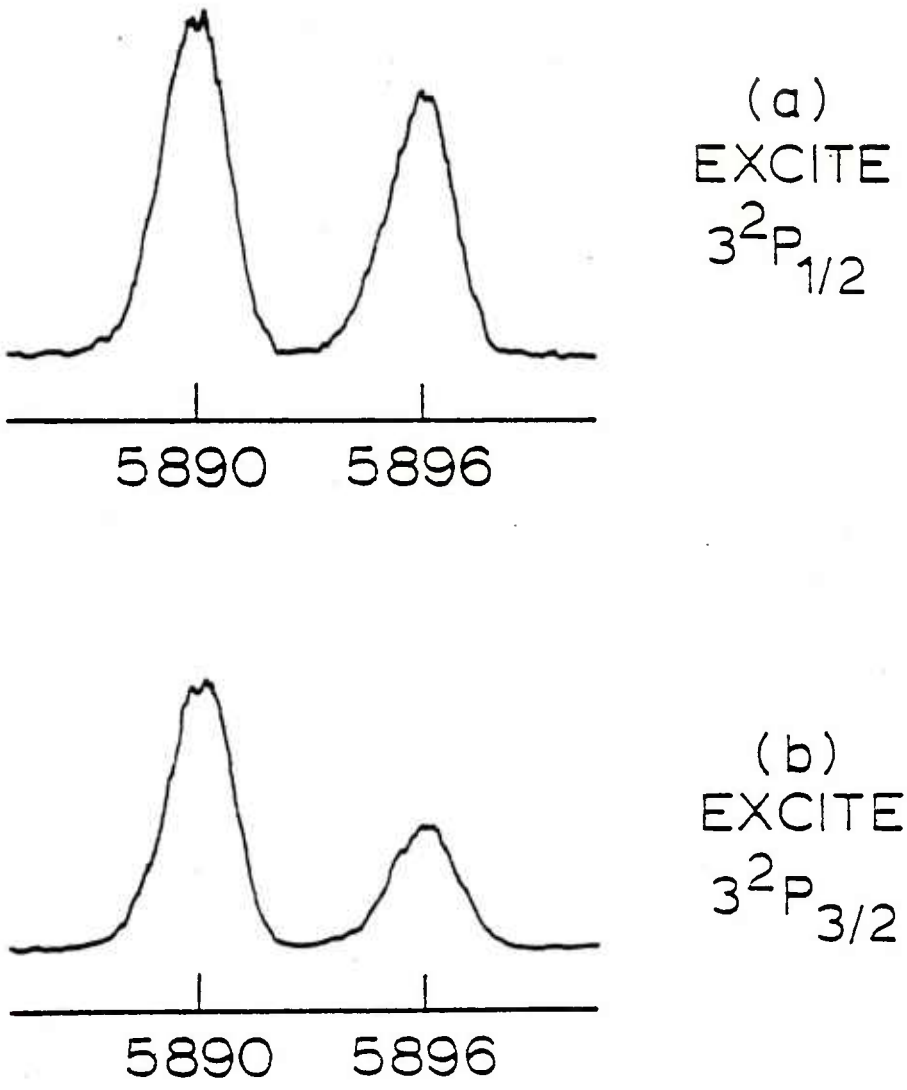

Figure 4. Spectrometer scans of the laser-induced fluorescence from the 3^2P levels, for excitation of level (3), the $^2P_{1/2}$ level at 5896A. The areas under these peaks are used to obtain the ratio R_3 and R_2.

several heights above the burner are listed in Table 5. It is immediately apparent that R_3 is closer to its computed thermal equilibrium value (0.48) than is R_2, whose equilibrium value is 1.98. This is a surprising result, and we have consequently carefully eliminated systematic errors due to self-absorption and scattered light. It suggests that $Q_{31} > Q_{21}$, so that the population accumulates in level 2 but not in level 3.

Figure 5 exhibits a plot of one experimental run in the form of Equation (5). Although the signal may be measured in arbitrary units, it is necessary to have the laser spectral power density I in absolute units in order to extract absolute rates. The values of T_{32}, Q_{31} and Q_{21} obtained from the slope-to-intercept ratios and Equations (3) through (5), are also given in Table 5 for several heights. (In this series, the results of the S^{-1} vs. I^{-1} runs at 2.0 cm are not self-consistent for unknown reasons, and have been excluded.)

Overall errors are difficult to assess in using this technique. We have found a systematic variation of measured quench rates with Na concentration at high concentration, although the runs listed in Table 5 were made at concentrations low enough that this should be no problem. There is also some variation with overall laser power (prior to insertion of the attenuating filter) which may be attributable to changes in the laser gain profile with power level. This parameter is constant enough here that we feel that the difference in experimental results between 1 and 3 cm is not an artifact of the experiment, although there remains investigation of the behavior of a highly quenched system under conditions of near optical saturation is needed to further establish this useful technique. In any case, the values of R_3 and R_2 themselves definitely indicate unequal quench rates in our flame.

In the experiments in which the 4p level was pumped using frequency doubled laser radiation, a search was made for the opto-acoustic pulse created by the collisional quenching of this state. None was found above the background noise level, at the microphone, of 0.2 mTorr pressure amplitude. Now in the case of the opto-acoustic pulse formed upon exciting 3P, reasonable agreement (a factor of two) was obtained between the measured absolute magnitude of the pressure wave, and that value calculated from the amount of translational heating using the (measured) laser energy absorbed per pulse.[3] Applying the same calculation to the 4P excitation, a pressure wave amplitude (as measured at the microphone) of 18 mTorr is anticipated. This surprising negative result indicates a different net electronic-to-translational energy conversion process at this higher energy. However, the general conclusions from Table 5 indicate that similar amounts of energy are transferred in single collisions from the Na to the flame gases, regardless of level. Thus the reason for the absence of the opto-acoustic pulses here is not a simple efficiency varying with energy, and we cannot offer a simple explanation.

TABLE 5. 3p QUENCHING AND TRANSFER RESULTS

HEIGHT ABOVE BURNER (cm)	R_3	R_2	SLOPE-TO INTERCEPT, LEVEL 3†	SLOPE-TO INTERCEPT RATIO LEVEL 2*	T^{**} $nsec^{-1}$	T^{***} $nsec^{-1}$	$T_{average}$ $nsec^{-1}$	Q_{31}† $nsec^{-1}$	Q_{21}† $nsec^{-1}$
1.0	0.472	1.30	0.0277	0.0513	6.0	6.7	6.4	3.3	0.82
1.5	0.481	1.34	0.0293	0.0532	7.1	7.7	7.4	3.5	0.69
2.0	0.483	1.34	0.0327	0.0188	-	-	-	-	-
3.0	0.470	1.37	0.0175	0.0357	4.3	5.1	4.7	2.0	0.63
AVERAGE ALL RUNS	0.476±0.007	1.34±0.03							

*Units: erg cm^{-2} sec^{-1} Hz^{-1}

**From level 3 pump

***From level 4 pump

†Using average T

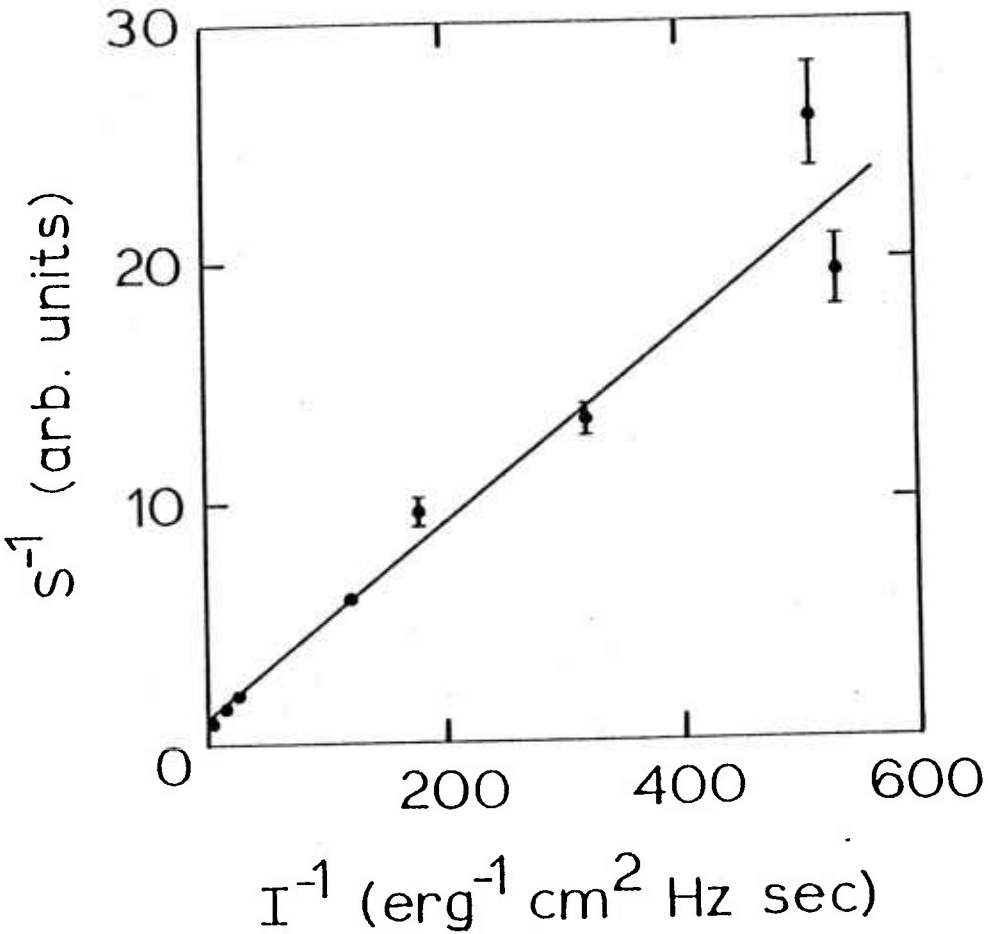

Figure 5. A plot of S_3^{-1} vs. I^{-1} as from Equation (4). The error bars are estimates from the raw data (where not shown, they are smaller than the points plotted). The straight line is a least squares fit. The errors for the two points at very low intensity (high I^{-1}) are probably underestimated due to drift in the laser; their exculsion here does not change the fitted parameters significantly but improves the standared deviations.

C. Linewidth Measurements

The absorption linewidths in this atmospheric pressure flame are caused by collisions of the electronically excited Na atoms with flame gases (Lorentz broadening). They should be larger than linewidths calculated simply from the measured total depopulation rates Q and transfer rate T, since the linewidth is affected by adiabatic phase-interrupting collisions as well.

Laser-excited fluorescence 'excitation scans' - in which the observation wavelength is held fixed while the laser is scanned across the absorption line - provide a convenient means of determining the pressure broadened linewidths, since resolution of the order of 0.1 cm^{-1} is easily attained with an intracavity etalon.

Excitation scans were made here using a linewidth of 0.33 cm^{-1}. Figure 6 shows the excitation spectrum for the $3^2P_{1/2}$ - $3^2S_{1/2}$ transition, with the spectrometer set to detect the collision-induced $3^2P_{3/2}$ - $3^2P_{1/2}$ emission (which directly tracks the amount of light absorbed and eliminates possible detection of scattered laser light). The data are fitted to a Lorentzian and the fit indicated in the figure. This run, as well as the others reported here, was carried out under conditions of low Na density and at a laser power below optical saturation.

It was necessary to consider the convolution of the laser linewidth with the absorption Lorentzian to obtain the collision width[7]. This does not significantly affect the 3P results (where $\Delta\nu_{Lor} \sim 5\Delta\nu_{laser}$) but is important for the 4D and 5S levels, and is responsible for the large error limits there. The width of the 4p level was consistent with the laser linewidth itself, which is 0.66 cm^{-1} in the ultraviolet. Also, the 3d excitation was too weak to yield a reliable linewidth. The results of these linewidth measurements at a height of 1 cm are collected in Table 6.

The measured linewidth of the $3^2P_{3/2}$ level is greater than that of $3^2P_{1/2}$, well outside experimental error. This result implies that the overall collision rate for the $3^2P_{3/2}$ level is larger than for the $3^2P_{1/2}$ level. Similarly, the quench rate Q_{31} has been shown in the preceding section to be substantially larger than Q_{21}. The problems discussed above in determining the absolute quench rates prohibit a direct comparison with the measured linewidth; however, these corresponding inequalities are certainly striking, although difficult to interpret.

---

[7] *H. G. Kuhn, Atomic Spectra, 2nd edition, p. 416, Academic Press, 1969.*

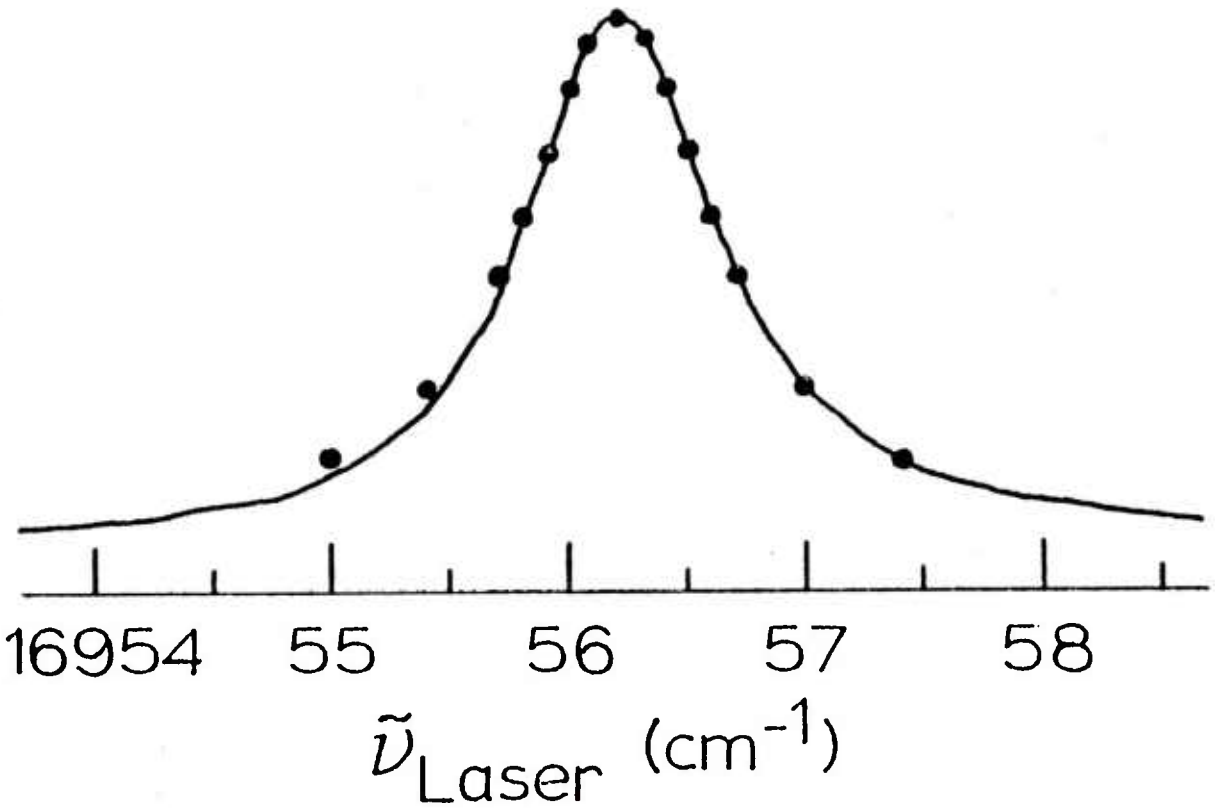

Figure 6. Excitation scan of $3^2P_{1/2}$ absorption line: fluorescence as a function of laser frequency. The points are the Lorentzian fit to the data.

TABLE 6. LINEWIDTH MEASUREMENTS

LEVEL	LINEWIDTH (FWHM) cm^{-1}	CORRESPONDING COLLISION RATE, $nsec^{-1}$
$3^2P_{3/2}$	1.08 ± 0.02	102 ± 2
$3^2P_{1/2}$	0.85 ± 0.02	80 ± 2
4^2D	0.12 ± .03	11 ± 3
5^2S	0.07 ± .03	7 ± 3

D. Sodium-Lithium Transfer

In this brief, and predominantly qualitative, series of experiments, the flame is seeded with an equimolar mixture of Na and Li. The laser is tuned to the Na 3p-3s transition and fluorescence is observed from both Na and from the Li 2p-2s transition. However, when the laser is tuned to the Li 2p-2s absorption, only a very small amount of emission can be observed from Na 3p-3s compared with that in the directly pumped Li.

Now the Na 3p level lies 2060 cm^{-1} higher than the Li 2p level. Were the transfer to occur in a direct manner

$$Na^* + Li = Li^* + Na \quad ,$$

detailed balancing predicts a ratio of Na emission to Li emission, for the Li-excited run, of well over ten times the observed value. Moreover, the alkali number densities are so low ($\sim 10^{11}$ cm^{-3}) that the Na-Li encounter rate is much less than the quench rate with the flame gases.

These results suggest, then, a net E→V→E transfer process with intermediate vibrational relaxation within the flame gases. The Na 3p electronic energy is removed by collisions with the flame gases (E→V). These molecules undergo some vibrational relaxation before encountering a Li atom, but still retain sufficient energy to significantly populate its 2p level (V→E). However, a similar degree of relaxation following deposition of the Li 2p electronic energy into the flame gases leaves too large an energy defect to appreciably populate Na 3p.

A similar mechanism has been invoked previously to explain Na to Cs excitation transfer in a bath of H_2 (at pressures of 0 to 50 torr), and to extract H_2 vibrational relaxation rates[8]. The use of a shorter laser pulse duration in the flame experiments may provide direct measurement relaxation times for vibrational energy in the flame medium.

III. DISCUSSION

We again note that our flame is not itself carefully enough characterized that one should draw detailed conclusions from the numerical results quoted. However, it is clear that the definite statements made in the earlier sections, concerning the general means by which energy is transferred throughout the network of Na energy levels, and the degree of equilibrium attained in these transfer processes, are valid.

---

[8] *D. A. Jennings, W. Braun and H. P. Broida, "Vibrational Relaxation of Hydrogen by Direct Detection of Electronic and Vibrational Energy Transfer with Alkali Metals" , J. Chem Phys. 59, 4305-4308 (1973).*

We briefly consider a comparison of our results with those of others in somewhat different experiments. Gallagher, Cooke and Edelstein[9] have used two-step pumping of Na 5s to obtain a few of the rates listed in Table 3 in collisions with N_2 at low pressure; we would expect some correspondence since our gases are largely N_2. It should be noted that they neglect the 4s level, as do we, and the 4d level as well as other upward transfer, which is less important in their room temperature experiment. Their $Q(5s)/Q(4p) = 2.0$ compares unfavorably with our equivalent $[Q(5s) - k(5s \rightarrow 4d)]/Q(4p) = 0.34$. However, the sum of their measured downward rates out of the 5s and 4p levels compares reasonably to our own (5s: 0.49 vs. 0.34; 4p: 0.44 vs. 0.42).

The possibility of differing quench rates for the two Na 3^2P components has to our knowledge received no direct investigation. For the corresponding level in Rb, the quench rates are the same for a number of gases[10]. For Cs-N_2 collisions, they are the same but the $^2P_{3/2}$ quench rate is nearly a factor of two larger than that for $^2P_{1/2}$ for Cs-H_2.[11]

Smith, Winefordner and Omenetto[12] have also investigated laser-excited fluorescence in Na 3p near optical saturation in an acetylene-air flame, for establishing detectability criteria for flame photometric measurements. They quote ratios corresponding to our R_3 of ~ 0.43 and for R_2 of ~ 1.6, which appears more consistent with equal quench rates. We do not understand the discrepancy.

Muller, Schofield and Steinberg[13] have found that the increase in net concentration of Na 3p under conditions of strong laser pumping leads to a net reactive loss of Na in an $H_2/O_2/N_2$ flame during the laser pulse.

---

[9] *T. F. Gallagher, W. E. Cooke and S. A. Edelstein, "Collisional Deactivation of the 5s and 4p States of Na by N_2", Phys. Rev. 17, 125-131 (1978).*

[10] *I. N. Siara and L. Krause, "Inelastic Collisions Between Excited Alkali Atoms and Molecules. VIII. $6^2P_{1/2}$ - $6^2P_{3/2}$ Mixing and Quenching in Mixtures of Rubidium with H_2, HD, D_2, N_2, CH_4, and CD_4", 257-265 (1973).*

[11] *D. A. McGillis and L. Krause, "Inelastic Collisions Between Excited Alkali Atoms and Molecules. I. Sensitized Fluorescence and Quenching in Cs-N_2 and Cs-H_2 Systems", Can. J. Phys. 46, 1051-1057 (1968).*

[12] *B. Smith, J. D. Winefordner, and N. J. Omenetto, "Atomic Fluorescence of Sodium Under Continuous-Wave Laser Excitation", Appl. Phys. 48, 2676-2680 (1977).*

[13] *C. H. Muller, III, K. Schofield, and M. Steinberg, "Laser-Induced Reactions of Sodium in Flames", American Chemical Society Meeting, Anaheim, CA, March 1978.*

Although important for considerations of the Na concentration throughout their flame, the reaction rates are much lower than our overall measured quench rates (assuming reasonable concentrations of H_2 and H_2O in our flame) and should not affect our results.

We compare our measured quench rates of $\sim$ 1-3 $nsec^{-1}$ for the 3p level with those calculated from bimolecular cross sections for the 3p doublet as a whole, obtained in a CH_4 flame.[14] The calculated result is 2.8 $nsec^{-1}$, suggesting that the measured quench rates are of the correct order of magnitude.

The conclusions and implications of these experiments, as they concern actual combustion processes, have already been described in the introduction and within the main body of the results. Finally, we note in addition that one can employ many modifications of this general technique of laser excitation of species in order to produce non-equilibrium populations within a flame. One possibility is direct pumping of reactants, using lasers in the infrared (for vibrational excitation) or visible/ultraviolet (for electronic excitation), together with a spectorscopic probing of the chemical consequences of such perturbations. This may be the most direct method to examine the effects of departures from thermal equilibrium on combustion chemistry.

---

[14] *H. P. Hooymayers and C. Th. J. Alkemade, "Quenching of Excited Alkali Atoms and Related Effects in Flames. Part II. Measurements and Discussions", J. Quant. Spect. Radiat. Transfer 6, 847-874 (1966).*

REFERENCES

1. A. G. Gaydon and H. G. Wolfhard, Flames, 3rd ed., Chapman and Hall, 1970.

2. P. R. Brooks and E. F. Hayes, editors, State-to-State Chemistry, Amer. Chem. Soc. Symposium Series 56, 1977.

3. J. E. Allen, W. R. Anderson, and D. R. Crosley, "Opto-Acoustic Pulses in a Flame", Optics Lett. 1, 118-120 (1977).

4. J. W. Daily, "Saturation Effects in Laser Induced Fluorescence Spectroscopy", Appl. Opt. 16, 568-571 (1977).

5. H. D. Zeman, Electron and Photon Interactions with Atoms, H. Kleinpoppen and M. R. C. McDowell, editors, p. 581, Plenum Press, 1976.

6. W. L. Wiese, M. W. Smith, and B. M. Miles, Atomic Transition Probabilities, Vol. II, p. 2, U.S. Government Printing Office, 1969.

7. H. G. Kuhn, Atomic Spectra, 2nd edition, p. 416, Academic Press, 1969.

8. D. A. Jennings, W. Braun, and H. P. Broida, "Vibrational Relaxation of Hydrogen by Director Detection of Electronic and Vibrational Energy Transfer with Alkali Metals", J. Chem. Phys. 59, 4305-4308 (1973).

9. T. F. Gallagher, W. E. Cooke, and S. A. Edelstein, "Collisional Deactivation of the 5s and 4p States of Na by N_2", Phys. Rev. 17, 125-131 (1978).

10. I. N. Siara and L. Krause, "Inelastic Collisions Between Excited Alkali Atoms and Molecules. VIII. $6^2P_{1/2}$-$6^2P_{3/2}$ Mixing and Quenching in Mixtures of Rubidium with H_2, HD, D_2, N_2, CH_4, and CD_4", 257-265 (1973).

11. D. A. McGillis and L. Krause, "Inelastic Collisions Between Excited Alkali Atoms and Molecules. I. Sensitized Fluorescence and Quenching in Cs-N_2 and Cs-H_2 Systems", Can. J. Phys. 46, 1051-1057 (1968).

12. B. Smith, J. D. Winefordner, and N. J. Omenetto, "Atomic Fluorescence of Sodium under Continuous-Wave Laser Excitation", Appl. Phys. 48, 2676-2680 (1977).

13. C. H. Muller, III, K. Schofield, and M. Steinberg, "Laser-Induced Reactions of Sodium in Flames", American Chemical Society Meeting, Anaheim, CA, March 1978.

14. H. P. Hooymayers and C. Th. J. Alkemade, "Quenching of Excited Alkali Atoms and Related Effects in Flames. Part II. Measurements and Discussions", J. Quant. Spect. Radiat. Transfer 6, 847-874 (1966).

DISTRIBUTION LIST

No. of Copies	Organization
12	Commander Defense Technical Info Center ATTN: DDC-DDA Cameron Station Alexandria, VA 22314
1	Director Defense Advanced Research Projects Agency ATTN: LTC C. Buck 1400 Wilson Boulevard Arlington, VA 22209
2	Director Institute for Defense Analysis ATTN: H. Wolfhard R. T. Oliver 400 Army-Navy Drive Arlington, VA 22202
1	Commander US Army Materiel Development and Readiness Command ATTN: DRCDMD-ST 5001 Eisenhower Avenue Alexandria, VA 22333
2	Commander US Army Armament Research and Development Command ATTN: DRDAR-TSS Dover, NJ 07801
5	Commander US Army Armament Research and Development Command ATTN: DRDAR-LCA, J. Lannon DRDAR-LC, T.Vladimiroff DRDAR-LCE, F. Owens DRDAR-SCA, L. Stiefel DRDAR-LC, D. Downs Dover, NJ 07801
1	Commander US Army Armament Materiel Readiness Command ATTN: DRSAR-LEP-L, Tech Lib Rock Island, IL 61299
1	Director US Army ARRADCOM Benet Weapons Laboratory ATTN: DRDAR-LCB-TL Watervliet, NY 12189
1	Commander US Army Watervliet Arsenal ATTN: Code SARWV-RD, R.Thierry Watervliet, NY 12189
1	Commander US Army Aviation Research and Development Command ATTN: DRSAV-E P. O. Box 209 St. Louis, MO 63166
1	Director US Army Air Mobility Research and Development Laboratory Ames Research Center Moffett Field, CA 94035
1	Commander US Army Communications Rsch and Development Command ATTN: DRDCO-PPA-SA Fort Monmouth, NJ 07703
1	Commander US Army Electronics Research and Development Command Technical Support Activity ATTN: DELSD-L Fort Monmouth, NJ 07703

DISTRIBUTION LIST

No. of Copies	Organization
1	Commander US Army Missile Command ATTN: DRSMI-R Redstone Arsenal, AL 35809
1	Commander US Army Missile Command ATTN: DRSMI-YDL Redstone Arsenal, AL 35809
1	Commander US Army Natick Research and Development Command ATTN: DRXRE, D. Sieling Natick, MA 01762
1	Commander US Army Tank Automotive Research & Development Cmd ATTN: DRDTA-UL Warren, MI 48090
1	Commander US Army White Sands Missile Range ATTN: STEWS-VT White Sands, NM 88002
1	Commander US Army Materials and Mechanics Research Center ATTN: DRXMR-ATL Watertown, MA 02172
3	Commander US Army Research Office ATTN: Tech Lib D. Squire F. Schmiedeshaff R. Ghirardelli M. Ciftan P. O. Box 12211 Research Triangle Park NC 27706
1	Director US Army TRADOC Systems Analysis Activity ATTN: ATAA-SL, Tech Lib White Sands Missile Range NM 88002
2	Office of Naval Research ATTN: Code 473 G. Neece 800 N. Quincy Street Arlington, VA 22217
1	Commander Naval Sea Systems Command ATTN: J.W. Murrin, SEA-62R2 National Center Bldg. 2, Room 6E08 Washington, DC 20360
1	Commander Naval Surface Weapons Center ATTN: Library Br., DX-21 Dahlgren, VA 22448
2	Commander Naval Surface Weapons Center ATTN: S. J. Jacobs, Code 240 Code 730 Silver Spring, MD 20910
1	Commander Naval Underwater Systems Cmd Energy Conversion Department ATTN: R.S. Lazar, Code 5B331 Newport, RI 02840
2	Commander Naval Weapons Center ATTN: R. Derr C. Thelen China Lake, CA 93555

DISTRIBUTION LIST

No. of Copies	Organization
1	Commander Naval Research Laboratory ATTN: Code 6180 Washington, DC 20375
3	Superintendent Naval Postgraduate School ATTN: Tech Lib D. Netzer A. Fuhs Monterey, CA 93940
2	Commander Naval Ordnance Station ATTN: A. Roberts Tech Lib Indian Head, MD 20640
3	AFOSR (B.T. Wolfson; D. Ball; L. Caveny) Bolling AFB, DC 20332
2	AFRPL (DYSC) ATTN: D. George J. N. Levine Edwards AFB, CA 93523
2	National Bureau of Standards ATTN: J. Hastie T. Kashiwagi Washington, DC 20234
1	Lockheed Palo Alto Rsch Labs ATTN: Tech Info Ctr 3521 Hanover Street Palo Alto, CA 94304
1	Aerojet Solid Propulsion Co. ATTN: P. Micheli Sacramento, CA 95813
1	ARO Incorporated ATTN: N. Dougherty Arnold AFS, TN 37389
1	Atlantic Research Corporation ATTN: M. K. King 5390 Cherokee Avenue Alexandria, VA 22314
1	AVCO Corporation AVCO Everett Research Lab Div ATTN: D. Stickler 2385 Revere Beach Parkway Everett, MA 02149
1	Foster Miller Associates, Inc. ATTN: A. J. Erickson 135 Second Avenue Waltham, MA 02154
1	General Electric Company Armament Department ATTN: M. J. Bulman Lakeside Avenue Burlington, VT 05402
1	General Electric Company Flight Propulsion Division ATTN: Tech Lib Cincinatti, OH 45215
2	Hercules Incorporated Alleghany Ballistic Lab ATTN: R. Miller Tech Lib Cumberland, MD 21501
1	Hercules Incorporated Bacchus Works ATTN: B. Isom Magna, UT 84044
1	IITRI ATTN: M. J. Klein 10 West 35th Street Chicago, IL 60615

DISTRIBUTION LIST

No. of Copies	Organization
1	Olin Corporation Badger Army Ammunition Plant ATTN: J. Ramnarace Baraboo, WI 53913
2	Olin Corporation New Haven Plant ATTN: R.L. Cook D.W. Riefler 275 Winchester Avenue New Haven, CT 06504
1	Paul Gough Associates, Inc. ATTN: P.S. Gough P. O. Box 1614 Portsmouth, NH 03801
1	Physics International Co. 2700 Merced Street Leandro, CA 94577
1	Pulsepower Systems, Inc. ATTN: L. C. Elmore 815 American Street San Carlos, CA 94070
3	Rockwell International Corp. Rocketdyne Division ATTN: C. Obert J. E. Flanagan A. Axeworthy 6633 Canoga Avenue Canoga Park, CA 91304
2	Rockwell International Corp. Rocketdyne Division ATTN: W. Haymes Tech Lib McGregor, TX 76657
1	Science Applications, Inc. ATTN: R. B. Edelman Combustion Dynamics and Propulsion Division 23146 Cumorah Crest Woodland Hills, CA 91364
1	Shock Hydrodynamics, Inc. ATTN: W. H. Anderson 4710-16 Vineland Avenue North Hollywood, CA 91602
1	Thiokol Corporation Elkton Division ATTN: E. Sutton Elkton, MD 21921
3	Thiokol Corporation Huntsville Division ATTN: D. Flanigan R. Glick Tech Lib Huntsville, AL 35807
2	Thiokol Corporation Wasatch Division ATTN: J. Peterson Tech Lib P. O. Box 524 Brigham City, UT 84302
1	TRW Systems Group ATTN: H. Korman One Space Park Redondo Beach, CA 90278
2	United Technology Center ATTN: R. Brown Tech Lib P. O. Box 358 Sunnyvale, CA 94088
1	Universal Propulsion Co. ATTN: H.J. McSpadden 1800 W. Deer Valley Road Phoenix, AZ 85027
11	Battelle Memorial Institute ATTN: Tech Lib R. Bartlett (10 cys) 505 King Avenue Columbus, OH 43201

DISTRIBUTION LIST

No. of Copies	Organization
1	Brigham Young University Dept of Chemical Engineering ATTN: M. W. Beckstead Provo, UT 84601
1	California Institute of Tech 204 Karmar Lab Mail Stop 301-46 ATTN: F.E.C. Culick 1201 E. California Street Pasadena, CA 91125
1	Case Western Reserve Univ. Division of Aerospace Sciences ATTN: J. Tien Cleveland, OH 44135
3	Georgia Institute of Tech School of Aerospace Eng. ATTN: B. T. Zinn E. Price W.C. Strahle Atlanta, GA 30332
1	Institute of Gas Technology ATTN: D. Gidaspow 3424 S. State Street Chicago, IL 60616
1	Johns Hopkins University/APL Chemical Propulsion Info Agency ATTN: T. Christian Johns Hopkins Road Laurel, MD 20810
1	Massachusetts Inst of Tech Dept of Mechanical Engineering ATTN: T. Toong Cambridge, MA 02139
1	Pennsylvania State University Applied Research Lab ATTN: G. M. Faeth P. O. Box 30 State College, PA 16801
1	Pennsylvania State University Dept of Mechanical Engineering ATTN: K. Kuo University Park, PA 16801
1	Pennsylvania State University Dept of Material Sciences ATTN: H. Palmer University Park, PA 16801
2	Princeton University Forrestal Campus ATTN: I. Glassman Tech Lib P. O. Box 710 Princeton, NJ 08540
2	Purdue University School of Mechanical Eng ATTN: J. Osborn S.N.B. Murthy TSPC Chaffee Hall West Lafayette, IN 47906
1	Rutgers State University Dept of Mechanical and Aerospace Engineering ATTN: S. Temkin University Heights Campus New Brunswick, NJ 08903
4	SRI International ATTN: Tech Lib D. Crosley J. Barker D. Golden 333 Ravenswood Avenue Menlo Park, CA 94025
1	Stevens Institute of Tech Davidson Library ATTN: R. McAlevy, III Hoboken, NJ 07030

DISTRIBUTION LIST

No. of Copies	Organization
1	University of California, San Diego Ames Department ATTN: F. Williams P. O. Box 109 La Jolla, CA 92037
1	University of Illinois Dept of Aeronautical Eng ATTN: H. Krier Transportation Bldg, Rm 105 Urbana, IL 61801
1	University of Minnesota Dept of Mechanical Eng. ATTN: E. Fletcher Minneapolis, MN 55455
1	University of Southern California Department of Chemistry ATTN: S. Benson Los Angeles, CA 90007
1	University of Texas Dept of Chemistry ATTN: W. Gardiner H. Schaefer Austin, TX 78712
2	University of Utah Dept of Chemical Engineering ATTN: A. Baer G. Flandro Salt Lake City, UT 84112
	Aberdeen Proving Ground Dir, USAMSAA ATTN: DRXSY-D DRXSY-MP, H. Cohen Cdr, USATECOM ATTN: DRSTE-TO-F Dir, USA CSL, Bldg. E3516 ATTN: DRDAR-CLB-PA